J Ther Eng, Vol. 7, No. 6, pp. 1329–1343, September, 2021

Journal of Thermal Engineering
Web page info: https://jten.yildiz.edu.tr
DOI: 10.18186/thermal.989993

Journal of Thermal Engineering

Research Article

Heat transfer analysis of hybrid active solar still with water flowing over glass cover

M.K. GAUR[1], G.N. TIWARI[2], Pushpendra SINGH[1,*], Anand KUSHWAH[3]

[1]Department of Mechanical Engineering, Madhav Institute of Technology & Science, Gwalior, India
[2]Research and Development Cell, SRM University, Lucknow, Uttar Pradesh, India
3Department of Mechanical Engineering, Delhi Technological University, Delhi, India

ARTICLE INFO

Article history
Received: 18 October 2019
Accepted: 26 December 2019

Key words:
PVT collector; Thermal efficiency; Hybrid active solar still; Thermal Modeling

ABSTRACT

The aim of this research is to carry out the heat transfer analysis of PVT hybrid active solar still (HASS) at different water depth to obtain maximum output. Experimentation is performed for validation of thermal modeling with and without flowing water, having water depth of 0.15m in the solar still basin. During experimentation, water flows above the glass cover. Theoretically calculated values of basin water, basin liner, glass temperature and yield obtained using thermal modeling are very near to the experimental values having correlation coefficients 0.988, 0.981, 0.999 and 0.985 respectively. It is also found that thermal efficiency and daily exergy output increases by 4% and 8.2% respectively for this hybrid system whose glass cover is getting cooled by water flowing over it. Theoretical calculation for distillate output of the system was also calculated out for various climatic conditions of India using developed thermal modeling and it is found that proposed system gives higher annual yield of 2756.67 kg/m^2 for the climate of Mumbai. The experimental uncertainty of the HASS is obtained as 14.82%.

Cite this article as: Gaur MK, Tiwari GN, Singh P, Kushwah A. Heat transfer analysis of hybrid active solar still with water flowing over glass cover. J Ther Eng 2021;7(6):1329–1343.

INTRODUCTION

Solar still consumes solar energy for producing fresh water from saline or impure water. As 97% of water is saline water available either in seas or oceans. Remaining water is locked in rivers, lakes and glaciers [1]. There is need of such system which can produce fresh water for huge population growth. In an every field, the solar energy is used as an alternative energy source [2,3]. For water purification, solar distillation system is found sustainable and it can be installed easily in remote/rural areas where availability of drinking water is poor [4]. Basically the solar stills are classified into active and passive types [5]. Active stills are better in terms of productivity than passive ones [6].

The innovative idea of utilizing thermal energy for evaporation of brine water and its consequent condensation for getting distilled water was traditionally in practice from

***Corresponding author.**
*E-mail address: pushpendra852@gmail.com, gmanojkumar@rediffmail.com

This paper was recommended for publication in revised form by Regional Editor Nader Javani

very ancient times. Telkes firstly described the accurate methodical relationship between the transports phenomena involved in the distillation process [7]. Digital simulation method was used by Cooper to analyze the solar still process [8]. In another work, he presented the highest theoretical efficiency of ideal basin type solar still up to 60% [9]. To evaluate the heat and mass transfer taking place inside the solar still, theoretical models and mathematical relations were firstly given by Dunkle (1961) [10]. The Dunkle's model was found accurate up to some extent beyond the yield of 0.1 g/m^{2}s, whereas the modified Dunkle's model gives over prediction of measurements at yield higher than 0.1 g/m^{2}s, this was also lately confirmed by Rahbar and Esfahani's CFD numerical investigation [11]. In early 1990's Malik et al. (1982) worked on solar still operating in passive mode [12]. Tiwari and Tiwari (2008) studied about the active and passive type of solar distillation systems pertaining rigorous analysis on performance evaluation and enhancement [13].

The difference in water and glass cover temperature mainly affects the amount of distillate collected. This can be increased either by

(i) Designing new system or using any external devices for increasing the temperature of water in basin.
(ii) Utilizing latent heat of vaporization of distilled water by double effect distillation or Regenerative effect.

Theoretical model was developed by Kumar and Tiwari for calculating daily output of active type double effect solar still. The performances of active type single and double-effect solar stills was also tested with and without flowing water over the glass cover during the peak summer [14,15].

Yousef et al. carried out the performance evaluation and modeling of regenerative type solar desalination unit [16]. They have considered a regenerative unit with two basins, having an arrangement for circulating cold water in and out through the second basin. They have also found that the output in case of regenerative still was obtained higher than the conventional still by 20%. During experimentation in air regenerative solar stills, thermal efficiency of passive type was observed better than active type and also in a solar distillation system attached with wind-driven aspirator, the thermal efficiency rises with rise in flow velocity of air [17]. The performance of regenerative type solar still was evaluated by Prakash and Kavathekar under ideal conditions [18]. The conclusions reported after parametric study of regenerative type active solar still are (i) Thermal efficiency of Passive stills was better than active ones and (ii) with rise in velocity of water, the thermal efficiency also rises [19]. Effect of thermal capacity on the performance of solar distillation system with water flowing above the glass cover was studied by Lawrence et al. [20]. The result showed that the efficiency of the solar still gets rises with increase in water flow rate over the glass cover. Singh and Tiwari studied the thermal performance of a regenerative type active solar still working on thermosyphonic effect in climate of Delhi [21]. It was observed that the overall performance improves significantly but regenerative effect had no impact on its yield. Performance of solar distillation system was enhanced by Bassam and Abu-Hijleh by cooling glass cover by using water film over it [22]. They have reported that suitable usage of water film over glass cover increases the still efficiency, but if poor combinations of parameters were taken it will results in reductions of still efficiency. Wibulswa and Tadtiam have reported rise in daily output of the solar still with regenerative effect on vertical wall [23]. Kudish have studied regenerative effect on glass cover of the solar distillation system [24]. The idea of flowing water over glass cover and at the back wall of the still and then recirculating this hot water inside the still was given by Wibulswa and Suntrirat [25].

Gugulothu et al. suggested that sensible and latent heat storage system can be used as association to overcome the gap between the energy sources, the sun and the desalination unit [26]. Effect of water depth was studied by Tiwari and Madhuri with transient analysis of a solar still [27]. The result showed that dependency of yield at certain water depth depends on the brine temperature. The daily output of the still gets increased when the brine initial temperature lies above 40°C and below 45°C. With advancement in the field of solar distillation a new concept of incorporation of flat plate collector/collectors and a pump to circulate water in solar still was developed to raise output of solar distillation systems. Hybrid systems can be used in remote/rural and this makes the system self-sustainable. P.T. Tsilingiris derived a set of expressions for calculating mass transfer coefficient based on the Bowen's ratio definition for application in solar stills which include Dunkle's mass transfer models [28]. Kumar and Tiwari estimated internal heat and mass transfer coefficients and analysed life cycle cost and exergy for HASS [29,30]. Using energy and exergy analysis, the number of solar collectors in HASS was optimized by Gaur and Tiwari for water with different heat capacity [31].

Singh and Tiwari studied solar still integrated with N identical PV/T compound parabolic concentrator and found 7 collectors were optimum for active solar distillation system with mass flow rate of 0.04 kg/s. Kabeel and Abdelgaied modified the solar still by integrating it with cylindrical parabolic concentrator, oil serpentine loop and phase change material under basin [32]. The mean daily efficiency of modified still was found 20.27% higher than conventional still. El-Sebaii and Naggar performed cost and annual performance analysis of single basin finned type solar distillation system using different fin materials [33]. They have also evaluated the experimental model showing improvement ratio of productivity (IRP) around 19% and improvement ratio of efficiency (IRE) 24% during winter

and summer and also shows finned-basin liner still are way better than conventional stills. Manokar et al. reviewed integrated PV/T solar still in comprehensive manner comparing performances of still in terms of yield along with considering testing place and latitude [34]. Kumar et al. analysed the impact of water mass on triangulated pyramid solar still attached with inclined solar still [35]. The study showed that maximum yield of 7.52 kg/m^2 was obtained from triangulated pyramidal solar still. The study on single slope active solar still coupled with two reflectors and PV/T system had also been done [36]. The setup was tested in climate of Ksar Challala, Algeria and the productivity was found increased in all seasons especially 127.06% in winter. Monthly performance of active and passive solar still for diverse climate was studied by Singh and Tiwari [37]. In order to get higher productivity from active solar still, absorber of porous nature with bubble wrap for insulation had been tested by Arunkumar et al. [38].

The present research focuses on the following objective:

- The validation of the developed thermal modeling, analysis of thermal efficiency and exergy analysis of the developed HASS.
- On the basis of developed thermal modeling, calculations of monthly and yearly yield for this modified solar distillation system is carried out in five zones of India namely New Delhi, Bangalore, Mumbai, Srinagar and Jodhpur having different climatic conditions.

Such kind of research has not been done before. The selection of these cities is made on the basis of divergence in their climatic conditions. The basically four types of weather conditions are shown in Table 1.

The data of average solar radiations in different climatic conditions has been taken from Indian Metrological Department (IMD), Pune.

EXPERIMENTAL SETUP

The HASS consists of one normal and one hybrid flat-plate collectors inclined at 45°, an arrangement for flowing water over glass surface, water storage tank and conventional solar still with cover inclination of 30°.

Figure 1(a) and 1(b) illustrates the cross-sectional side and pictorial view of HASS respectively. Both the collectors are attached in series to obtain maximum basin water temperature. A semi-transparent glass to glass PV module of 70 W_p is attached on partial surface of first flat-plate collector to generate D.C. power for operating the pump which circulates water from solar still to flat-plate collector. A 1.2 m length and 0.0127m diameter fiber plastic pipe having small-small holes throughout entire length is provided at the top height of the solar still for flowing water over the cover. Flow of the water is maintained through control valve. A proper arrangement has been made for outlet of the water flowing above the glass cover.

THERMAL MODELING

The assumptions considered during the thermal modeling of the integrated HASS are:

- Quasi state/ steady state heat transfer.
- Proper insulation is provided in all connecting pipes.
- Heat capacity of insulating and absorbing material is considered negligible.
- System is leak proof.
- In comparison to basin area, side area is very small.
- Uniform temperature of water mass.
- The ohmic losses in the PV module are considered negligible.
- Neglecting the thermal storage of water film above the glass cover due to thin film and high flow velocity.
- $T_{gi} = T_{go} = T_g$

PVT Collectors Connected in Series

For PV module and collectors, useful heat output is given as [39]:

Rate of useful thermal energy available at the outlet of the PV and PVT collectors = (Total solar thermal energy absorbed by both the collectors) – (Heat loss from absorber plates and solar cell to ambient)

$$\begin{aligned}\dot{Q}_{u,(m+c_1+c_2)} = &\Big[A_m F_{Rm} PF_2 (\alpha\tau)_{m,eff} (1-K_1) \\ &+ A_{c1} F_{Rc1} (\alpha\tau)_{c1,eff} (1-K_2) \\ &+ A_{c2} F_{Rc2} (\alpha\tau)_{c2,eff} (1-K_1) \Big] I'(t) \\ -&\Big[A_m F_{Rm} U_{L,m} (1-K_1) + A_{c1} F_{Rc1} U_{L,c1} (1-K_2) \\ &+ A_{c2} F_{Rc2} U_{L,c2} \Big] (T_{fi} - T_a)\end{aligned} \quad (1)$$

Table 1. Different weather conditions with basis on which they are classified

Condition	Weather	Ratio of Daily diffused to Daily global radiation	Sunshine Hours
I	Clear day (blue sky)	Less than 0.25	More than 9 hours
II	Hazy day (fully)	0.25 – 0.50	7 – 9 hours
III	Hazy and Cloudy (partially)	0.50 – 0.75	5 – 7 hours
IV	Cloudy (fully)	More than 0.75	Less than 5 hours

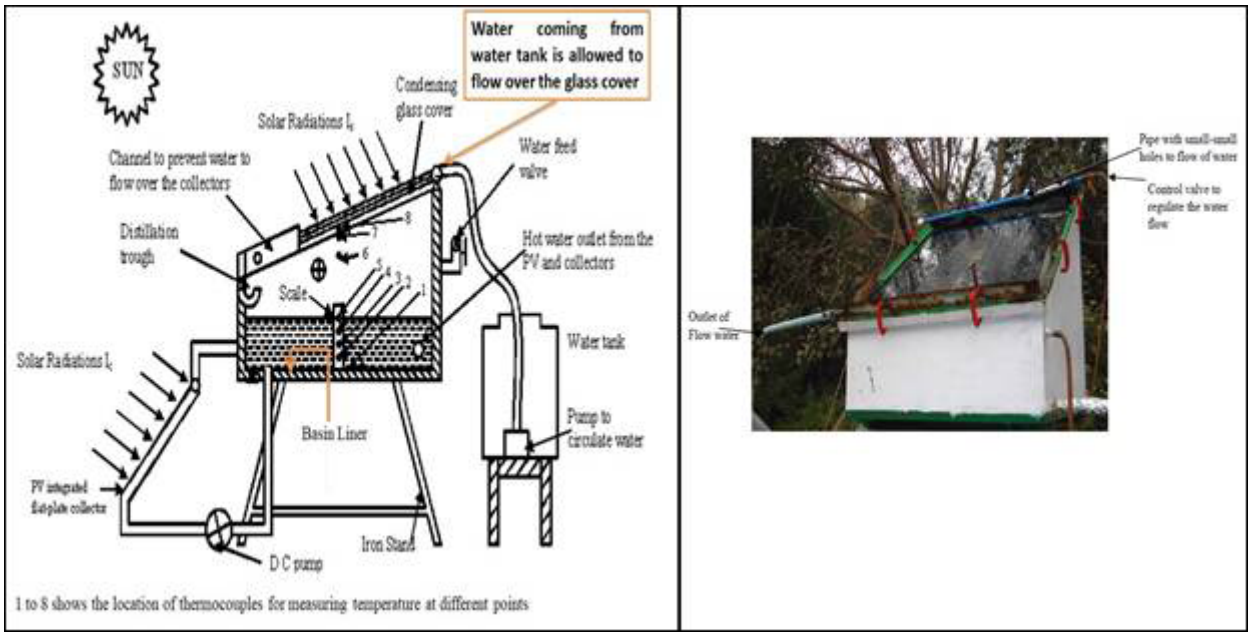

(a)

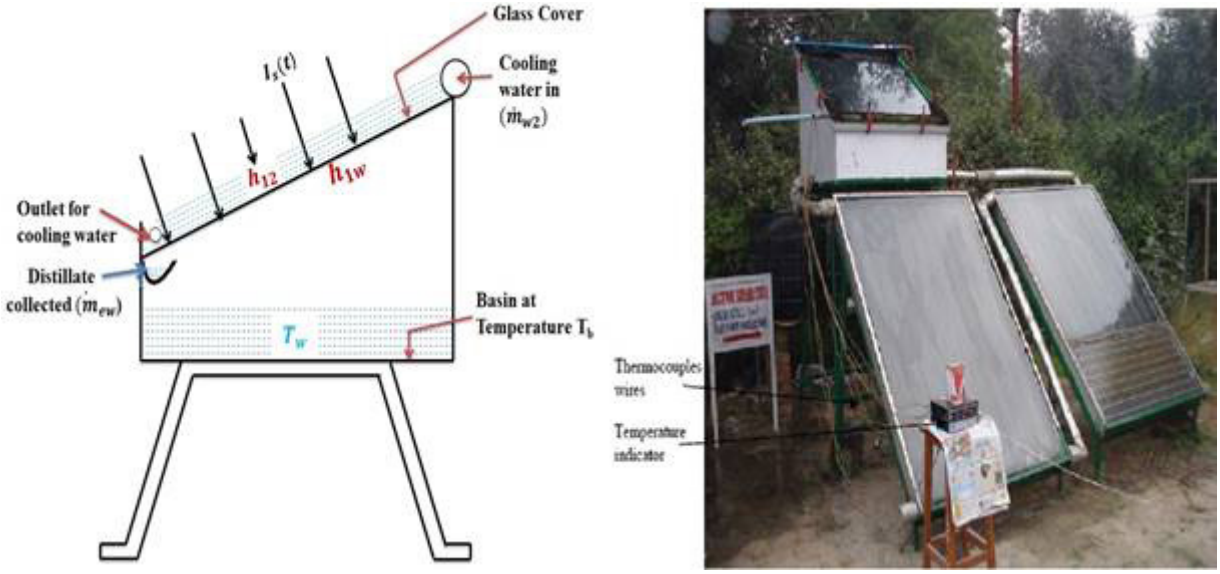

(b)

Figure 1. (a) Schematic diagram of Side view of hybrid solar still with water flow over the glass surface. (b) Developed Hybrid solar still with water flow over the glass surface.

where,

$$K_1 = \left(\frac{A_{c1}F_{Rc1}U_{L,c1}}{\dot{m}_f C_f} + \frac{A_{c2}F_{Rc2}U_{L,c2}}{\dot{m}_f C_f} - \frac{A_{c1}F_{Rc1}U_{L,c1} \cdot A_{c2}F_{Rc2}U_{L,c2}}{\left(\dot{m}_f C_f\right)^2} \right)$$

and

$$K_2 = \left(\frac{A_{c2}F_{Rc2}U_{L,c2}}{\dot{m}_f C_f} \right)$$

Energy Balance in HASS with Water Flowing over Glass Cover:

(i) Basin liner

$$A_b \alpha'_w I_s(t) = h_{bw}(T_b - T_w)A_b + h_{ba}(T_b - T_a)A_b \qquad (2a)$$

The expression of the T_b can be written from the above equation as:

$$T_b = \frac{\alpha'_b I_s(t)A_b + h_{bw}T_w A_b + h_{ba}T_a A_b}{h_{bw} + h_{ba}} \qquad (2b)$$

(ii) Water mass

For water mass inside still, energy balance equation is given by:

$$\dot{Q}_{u,(m+c_1+c_2)} + A_b\alpha'_w I_s(t) + h_{bw}(T_b - T_w)A_b = M_w C_w \frac{dT_w}{dt} + h_{1w}(T_w - T_g)A_b \quad (3)$$

(iii) Glass cover

$$\alpha'_g I_s(t)A_g + h_{1w}(T_w - T_g)A_b = h_{12}(T_g - \overline{T}_{w2})A_g \quad (4a)$$

The expression of T_g can be written from the above equation as:

$$T_g = \frac{\alpha'_g I_s(t)A_g + h_{1w}(T_w - T_g)A_b + h_{12}\overline{T}_{w2}A_g}{h_{12}A_g + h_{1w}A_b} \quad (4b)$$

(iv) Water mass flowing above the glass surface:

Consider a small thickness (dx) of water film flowing over the glass cover as illustrated in **Figure 2**.

The energy balance for small area (bdx) of water film can be given as:

$$h_{12}(T_g - T_{w2})b \times dx = \dot{m}_{w2}C_w\left(\frac{dT_{w2}}{dx}\right)\times dx + h_{1w2}(T_{w2} - T_a)b \times dx \quad (5)$$

Solving the above equation for the average water temperature. The Eq. (5) becomes:

$$\left(\frac{dT_{w2}}{dx}\right) + a_1 T_{w2} = f_1(t) \quad (6)$$

where,

$$f_1(t) = \frac{(h_{12}T_g + h_{1w2}T_a)\times b}{\dot{m}_{w2}C_w} \text{ and } a_1 = \frac{(h_{1w2} + h_{12})b}{\dot{m}_{w2}C_w}$$

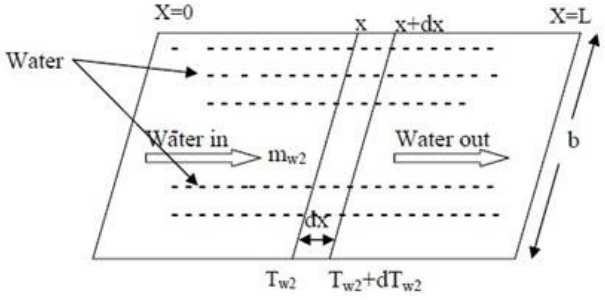

Figure 2. Cross-sectional view of elementary length of flowing water over the glass surface.

Following assumptions are considered to get approximate solution of Eq. (6):

- Initially at $x = 0$, $T_{w2} = T_{w2i} = T_a$
- $f(t)$ is considered constant at any time interval Δt i.e. $f_1(t) = \bar{f}_1(t)$.
- At any time interval Δt, a_1 is also constant.

Now, the solution of Eq. 6 is gives by:

$$T_{w2} = \frac{\overline{f_1}(t)}{a_1}\left(1 - e^{-a_1 x}\right) + T_{w2i}e^{-a_1 x} \quad (7)$$

Since the length of condensing cover is about 1m (small) and mass flow rate $\dot{m}_{w2}$ over the glass cover is large (0.058 kg/sec) and hence there will be not much variation in T_{w2} with x.

After integrating above equation for the entire length of the cover, the Eq. (7) becomes:

$$\overline{T}_{w2} = \left(\frac{\overline{f_1}(t)}{a_1}\right)\left(1 - \left(\frac{1 - e^{-a_1 L}}{a_1 L}\right)\right) + T_a\left(\frac{1 - e^{-a_1 L}}{a_1 L}\right)$$

Here, $T_{w2i} = T_a$

Or

$$\overline{T}_{w2} - T_a = \left(\frac{\overline{f_1}(t)}{a_1} - T_a\right)\left(1 - \left(\frac{1 - e^{-a_1 L}}{a_1 L}\right)\right) \quad (8)$$

After putting the values of T_g and T_b in Eq. (3), we will get:

$$\dot{Q}_{u,(m+c_1+c_2)} + A_b\alpha'_w I_s(t) = M_w C_w \frac{dT_w}{dt} - \left[\left(\frac{A_b\alpha'_g h_{1w}A_g}{h_{12}A_g + h_{1w}A_b}\right) + \left(\frac{A_b\alpha'_b h_{bw}}{h_{ba} + h_{bw}}\right)\right]I(t) + A_b\left[\left(\frac{h_{12}A_g h_{1w}}{h_{12}A_g + h_{1w}A_b}\right) + \left(\frac{h_{ba}h_{bw}}{h_{ba} + h_{bw}}\right)\right](T_w - T_a) - \left(\frac{h_{1w}A_b h_{12}A_g}{h_{12}A_g + h_{1w}A_b}\right)(\overline{T}_{w2} - T_a)$$

or,

$$\dot{Q}_{u,(m+c_1+c_2)} + \left[\alpha'_w + \left(\frac{\alpha'_g h_{1w}A_g}{h_{12}A_g + h_{1w}A_b}\right) + \left(\frac{\alpha'_b h_{bw}}{h_{ba} + h_{bw}}\right)\right]A_b I_s(t) + \left(\frac{h_{1w}A_b h_{12}A_g}{h_{12}A_g + h_{1w}A_b}\right)(\overline{T}_{w2} - T_a) = M_w C_w \frac{dT_w}{dt} + A_b\left[\left(\frac{h_{12}A_g h_{1w}}{h_{12}A_g + h_{1w}A_b}\right) + \left(\frac{h_{ba}h_{bw}}{h_{ba} + h_{bw}}\right)\right](T_w - T_a)$$

or,

$$\dot{Q}_{u,(m+c_1+c_2)}+\left[\alpha_w'+\alpha_g'h_1A_g+h_1\alpha_b'\right]A_bI_s(t) +(UA)_g(\overline{T}_{w2}-T_a)=M_wC_w\frac{dT_w}{dt}+(UA)_s(T_w-T_a) \quad (9)$$

Substituting the value of $\dot{Q}_{u,(m+c_1+c_2)}$ and $\left(\overline{T}_{w2}-T_a\right)$ in the above equation. Then Eq. (9) becomes:

$$\left[\left(A_mF_{Rm}PF_2(\alpha\tau)_{m,eff}(1-K_1)+A_{c1}F_{Rc1}(\alpha\tau)_{c1,eff}(1-K_2) +A_{c2}F_{Rc2}(\alpha\tau)_{c2,eff}\right)I'(t)+(\alpha'_{eff})A_bI(t)\right]= M_wC_w\frac{dT_w}{dt}+\left[A_mF_{Rm}U_{L,m}(1-K_1)+A_{c1}F_{Rc1}U_{L,c1}(1-K_2)\right. \quad (10) +A_{c2}F_{Rc2}U_{L,c2}+(UA)_s\left](T_w-T_a)\right. -(UA)_g\left(\frac{\overline{f}_1(t)}{a_1}-T_a\right)\left(1-\left(\frac{1-e^{-a_1L}}{a_1L}\right)\right)$$

If we assume,

$$(IA)_{eff}=\left[\left(A_mF_{Rm}PF_2(\alpha\tau)_{m,eff}(1-K_1)+A_{c1}F_{Rc1}(\alpha\tau)_{c1,eff}(1-K_2) +A_{c2}F_{Rc2}(\alpha\tau)_{c2,eff}\right)I'(t)+\left(\alpha'_{eff}\right)A_bI(t)\right] +(UA)_g\left(\frac{\overline{f}_1(t)}{a_1}-T_a\right)\left(1-\left(\frac{1-e^{-a_1L}}{a_1L}\right)\right)$$

and

$$(UA)_{eff}=\left[A_mF_{Rm}U_{L,m}(1-K_1)+A_{c1}F_{Rc1}U_{L,c1}(1-K_2) +A_{c2}F_{Rc2}U_{L,c2}+(UA)_s\right]$$

then Eq. (10) becomes:

$$(IA)_{eff}=M_wC_w\frac{dT_w}{dt}+(UA)_{eff}(T_w-T_a)$$

The solution of above differential equation is given as

$$\frac{dT_w}{dt}+\frac{(UA)_{eff}}{M_wC_w}T_w=f_2(t)$$

$$\frac{dT_w}{dt}+a_2T_w=f_2(t) \quad (11)$$

$$a_2=\frac{(UA)_{eff}}{M_wC_w}\text{ and }f_2(t)=\frac{(IA)_{eff}+(UA)_{eff}T_a}{M_wC_w}$$

Following assumptions are considered to get solution of the equation (11):

- $f_2(t)$ is considered constant at any time interval Δt i.e. $f_2(t)=\bar{f}_2(t)$.
- At any time interval Δt, a_2 is also constant.

Solution of Eq. (11) is written as:

$$T_w=\frac{\overline{f}_2(t)}{a_2}\left(1-e^{-a_2t}\right)+T_{wo}e^{-a_2t} \quad (12)$$

Where, T_{wo} = Basin Temperature when $t = 0$
$\bar{f}_2(t)$ = Mean value of $f_2(t)$ during time interval 0 and t.

In this experiment, $t = 3600$ sec.
The rate of evaporative heat transfer is calculated using:

$$\dot{q}_{ew}=h_{ew}(T_w-T_g) \quad (13)$$

The rate at which water evaporates in the still is given by:

$$\dot{m}_{ew}=\frac{\dot{q}_{ew}}{L} \quad (14)$$

Exergy Analysis

According to II[nd] law of thermodynamics, the exergy analysis of the solar still includes the total exergy inflow, outflow and destructed [40].

$$\sum\dot{E}x_{in}-\sum\dot{E}x_{out}=\sum\dot{E}x_{dest} \quad (15)$$

Where, $\Sigma\dot{E}x_{in}$ = exergy input,
$\Sigma\dot{E}x_{out}$ = exergy output and
$\Sigma\dot{E}x_{dest}$ = exergy destructed
Exergy output from a solar still is given by:

$$\sum\dot{E}x_{out}=A_b\times\dot{q}_{ew}\times\left(1-\frac{T_a+273}{T_w+273}\right) \quad (16)$$

For solar still, Exergy input is summation of exergy input of solar still, PVT collector, collector and pump, and is given by:

$$\sum\dot{E}x_{in}=\sum\dot{E}x_{in}(solar\ still)+\sum\dot{E}x_{in}\left[\left(\frac{PV}{T}\right)FPC\right] +\sum\dot{E}x_{in}(FPC)+\sum\dot{E}x_{in}(Pump) \quad (17)$$

The exergy input to PVT collector and collector is given as [41]:

$$\sum\dot{E}x_{in}\left[\left(\frac{PV}{T}\right)FPC\right]= A_{(c+m)}\times\sum I'(t)\times\left[1-\frac{4}{3}\times\left(\frac{T_a+273}{T_s}\right)+\frac{1}{3}\times\left(\frac{T_a+273}{T_s}\right)^4\right]$$

and,

$$\sum \dot{E}x_{in}\left(FPC\right)= A_{(c)}\times\sum I'(t)\times\left[1-\frac{4}{3}\times\left(\frac{T_a+273}{T_s}\right)+\frac{1}{3}\times\left(\frac{T_a+273}{T_s}\right)^4\right]$$

The exergy input of the pump is given as:

The wattage of the pump (in this case the wattage of pump is 40W for 8 feet height)

For solar still the exergy input given by:

$$\sum \dot{E}x_{in}\left(solar\ still\right)= A_b\times\sum I(t)\times\left[1-\frac{4}{3}\times\left(\frac{T_a+273}{T_s}\right)+\frac{1}{3}\times\left(\frac{T_a+273}{T_s}\right)^4\right] \quad (18)$$

Overall Efficiencies of Regenerative HASS

Overall thermal efficiency of the HASS is given by:

$$\eta_{th}=\frac{\left(\sum \dot{m}_{ew}\times L\right)}{\left[\left(A_b\sum I_s(t)\right)+\left(A_{(c_1+m+c_2)}\times\sum I'(t)\right)+wattage\ of\ pump\times running\ hours\right]\times\Delta t}\times 100 \quad (19)$$

The overall exergy efficiency of still is calculated by:

$$\eta_{\dot{E}x}=\frac{Exergy\ output\ of\ solar\ still\left(\sum \dot{E}x_{out}\right)}{Exergy\ input\ of\ solar\ still\left(\sum \dot{E}x_{in}\right)}$$

$$\eta_{\dot{E}x}=1-\frac{\sum \dot{E}x_{dest}}{\sum \dot{E}x_{in}}\ \text{or}\ \frac{\sum \dot{E}x_{dest}}{\sum \dot{E}x_{in}} \quad (20)$$

Exergy destruction ($\dot{E}x_{dest}$) inside a solar still is given by:

$$\sum \dot{E}x_{dest}=M_w\times C_w\times(T_w-T_{gi})\times\left(1-\frac{T_a+273}{T_w+273}\right)\times(A_b+A_s) \quad (21)$$

METHODOLOGY

Experimental Procedure and Observations

The experiments were conducted on November 19 and 20, 2018, with and without water flowing above the glass cover of the HASS having 0.15 m water depth in the basin. To maintain the quasi-steady state condition, the solar still is to be filled with 150 liters of water in 24 hours before the commencement of the experiment. Water is allowed to flow at constant rate above the glass surface of the still by using control valve from 9 am to 5 pm.

The experiment was carried out for 24 hours i.e. from 8 am of 19 Nov to 8 am of 20 Nov 2018 (local time of New Delhi). Various parameters were measured hourly for different water depth like Temperature of Basin liner (T_b), Inner glass (T_{gi}), Outer glass (T_{go}), Vapour temperature (T_v), Water Temperature (T_w) at different depth, Ambient temperature (T_a), Total incident radiation, Hourly distillate yield, Wind velocity (V_a), etc. The various design parameters of the experimental setup are shown in Table 2.

Experimental Uncertainty

The accuracy of the measured data is validated by calculating the uncertainty in the measured data. Uncertainty analysis provides the error possible in the values measured by using a certain instrument. The accuracy and standard uncertainty are given by Table 3. The standard uncertainty is calculated by Eq. 22 given as,

$$Standard\ Uncertainty\ (\sigma)=\frac{Accuracy\ of\ instrument}{\sqrt{3}} \quad (22)$$

Experimental uncertainty has been calculated by taking the square root of the summation of individual standard uncertainties divided by square of number of samples taken. The internal uncertainty (U) is given by Eq. (23) as follows [42],

$$U=\sqrt{\frac{\sigma_1^2+\sigma_2^2+\sigma_3^2+\ldots+\sigma_n^2}{N^2}} \quad (23)$$

Table 2. Design parameters of photovoltaic module, flat-plate collector and solar still

Parameters	Value	Parameters	Value
A_m	0.66 m^2	A_b	1 m^2
F'	0.8	M_w	150 kg
$(\alpha\tau)_{m,\,eff.}$	0.304	$C_f = C_w$	4190 kJ/kg°C
F_{Rm}	0.95	h_{1s}	5.7+3.8 V_a, here V_a =1 m/s
U_{Lm}	2.074	L	2.25×10^5 J/kg
$PF2$	0.979	t	3600 sec
Solar cells in PV Module	36	$\propto'_g$	0.05
A_{c1} of first collector	1.34 m^2	$\propto'_w$	0.34
A_{c2} of second collector	2.0 m^2	$\propto'_b$	0.36
$U_{Lc1} = U_{Lc2}$	5 W/m^2°C	L_g	0.004 m
h_{12}	100 W/m2°C	kg	0.78 W/m°C
$(\alpha\tau)_{c1,eff} = (\alpha\tau)_{c2,eff}$	0.8	d_p	0. 0127 m
$F_{Rc1} = F_{Rc2}$	0.9	L_p	1.2 m

Table 3. Technical specification of the instruments used in the experiments

Instruments Used	Accuracy	Range	Standard Uncertainty (σ)
Thermocouple	±0.625°C	0 to 100 °C	0.3608 °C
Thermometer	±0.5°C	0 to 100 °C	0.288 °C
Solarimeter (Central Electronic Limited (CEL), India)	±1 W/m²	0–1200 W/m²	0.577 W/m²
Anemometer (LUTRON AM-4201)	±0.1 m/s	0–45 m/s	0.0577 m/s
Stop Watch	±0.015 min	60 minutes	0.0087 min

The total experimental uncertainty for hybrid active solar still has been calculated as 14.82%.

Theoretical Observations

Data collected from IMD (Indian meteorological department) Pune have been used for the theoretical calculations. Following steps are used for computing the hourly values various temperature i.e. basin liner, basin water temperature, glass surface temperature and yield:

i) Initially when $t = 0$, the temperature of basin water (T_{wo}) and inner glass (T_{gi}) are observed. Total internal heat transfer coefficient was calculated for different temperature, design and other climatic parameters. After calculating the value of total internal heat transfer coefficient, the value of still water temperature (T_w) is also calculated at time t using Eq. 12. Using T_w, the values of T_g and T_b are evaluated and then hourly yield is obtained using Eqs. 13–14.

ii) Now by using Eq. 8, the value of average water temperature ($\bar{T}_{w2}$) has been calculated. After getting the value of ($\bar{T}_{w2}$) the new value of water temperature (T_w) and hourly yield at time t is calculated.

iii) The step I and II are repeated to calculate all heat transfer coefficients and yield on hourly basis for a day.

iv) Thermal efficiency and exergy analysis for HASS with and without water flowing over the glass cover were calculated using Eqs. (19–20).

The value of $\bar{T}_{w2}$ is calculated from 9 am to 5 pm only. The value of $\bar{T}_{w2}$ used in all calculations between 6 pm to morning 8 am has been taken as zero (i.e. no water flow above the glass cover). Algorithm MATLAB 7 is used for numerical computation.

RESULTS AND DISCUSSION

The hourly variation in solar intensity with ambient air temperature on a typical day of Nov.19 is illustrated in Figure 3.

Figure 4a–c show the hourly variation of calculated and observed values of basin liner, basin water and glass temperature of HASS with water flowing over glass cover for the typical day of November month for the composite condition of Delhi climate. All Figures show good agreement of theoretical results with the experimental results.

Variation in theoretical and experimental values of yield per hour is given in Figure 5. Figure shows close agreement of theoretical value of yield with the experimental value with correlation factor of 0.985. Figure 6 illustrates the hourly change in yield with and without water flowing over the glass cover of the HASS. The higher yield is obtained in case of HASS is due to the fact that with flow of water above the

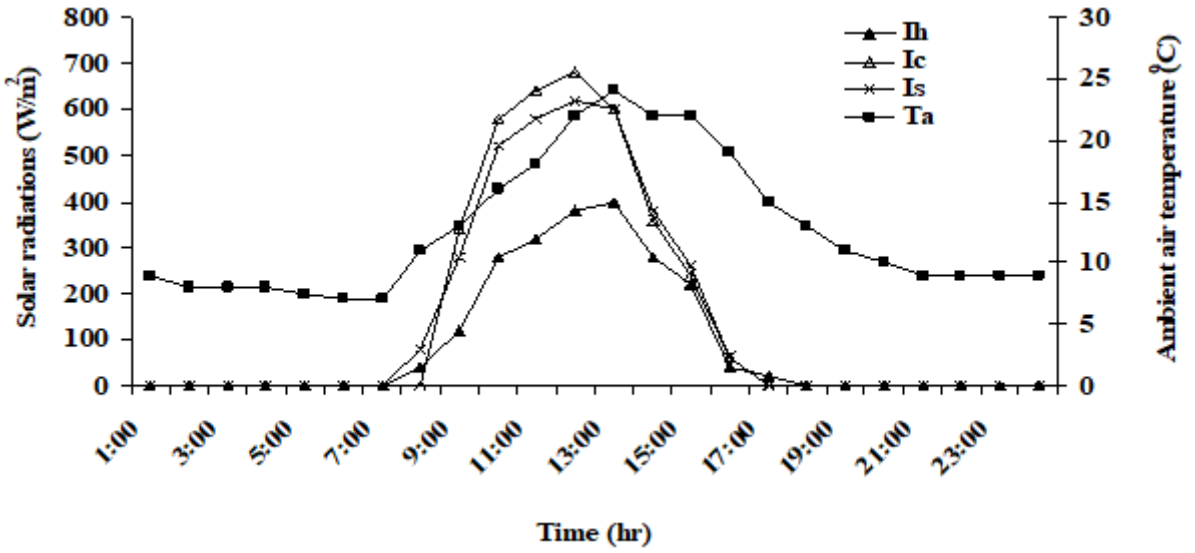

Figure 3. Hourly variation of solar intensity on horizontal plane, flat plate collector, and solar still and ambient temperature.

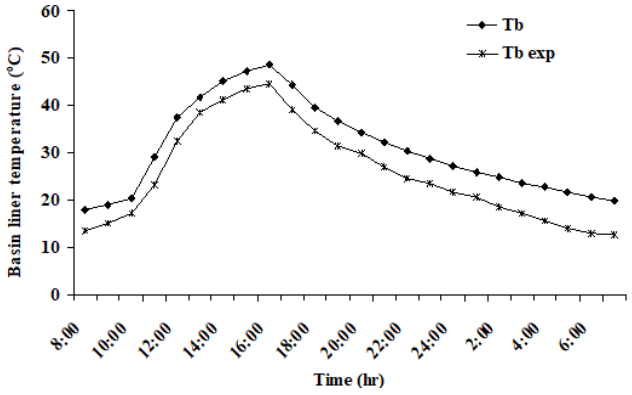

(a)

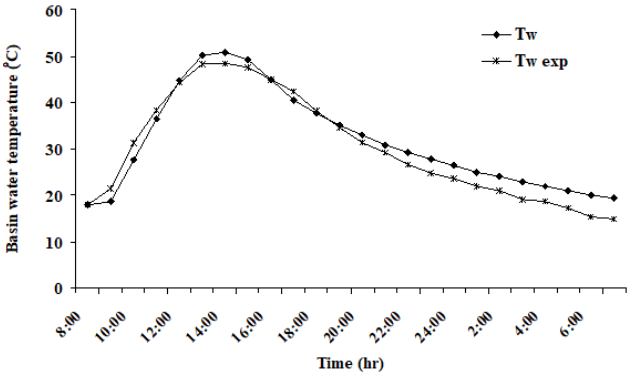

(b)

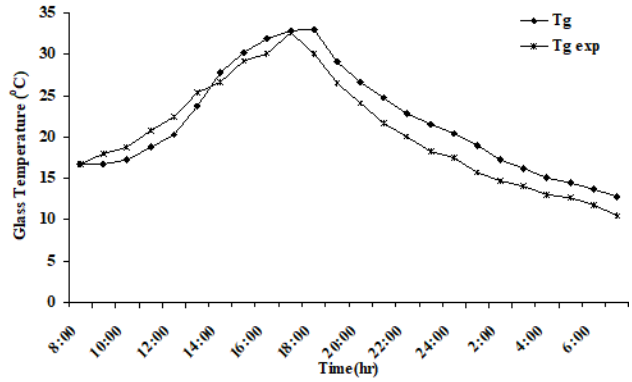

(c)

Figure 4. (a) Hourly variation of theoretical and experimental values of basin liner temperature (With water flow). (b) Hourly variation of theoretical and experimental values of basin water temperature (With water flow). (c) Hourly variation of theoretical and experimental values of glass temperature (With water flow).

glass surface the liberation of latent heat of condensation of water vapour becomes faster and hence a higher yield. The hourly yield curves for with and without water flow overlaps each other at night. This is because of the fact that the water flowing above the glass surface is stopped at 5:00 p.m.

Variation of daily efficiency has been shown in Figure 7. Figure shows that the daily efficiency of HASS is higher in

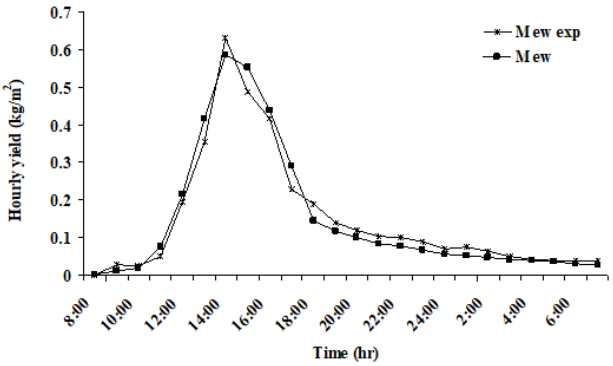

Figure 5. Hourly variations of theoretical and experimental values of yield (With water flow).

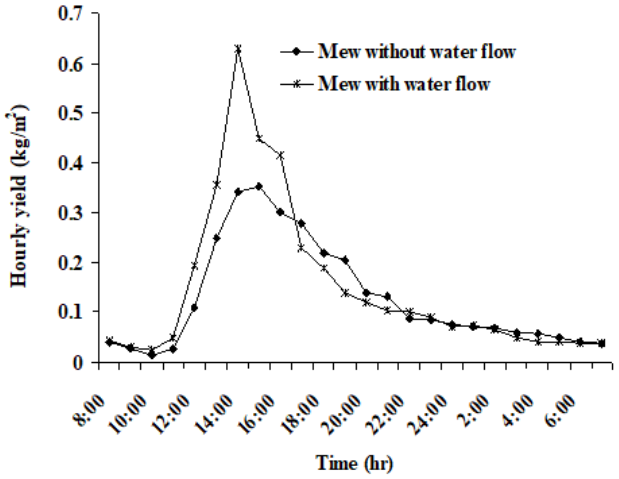

Figure 6. Hourly variation of yield with and without water flow.

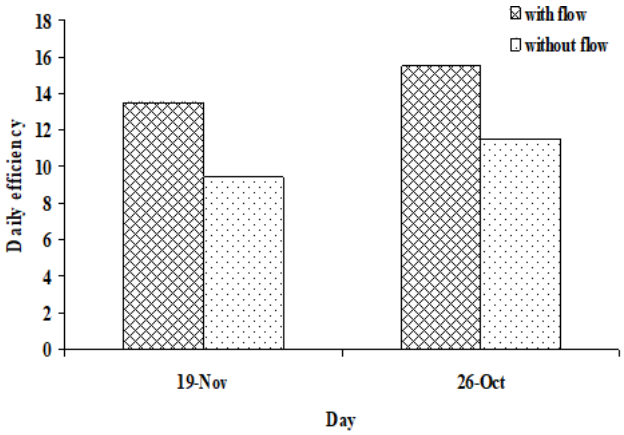

Figure 7. Variation of daily efficiency with and without water flow.

case of water flowing over the glass surface. It is found that the efficiency for the HASS with water flow is 4% higher than the without water flow. The variation of hourly exergy and analysis of daily exergy with and without water flow for

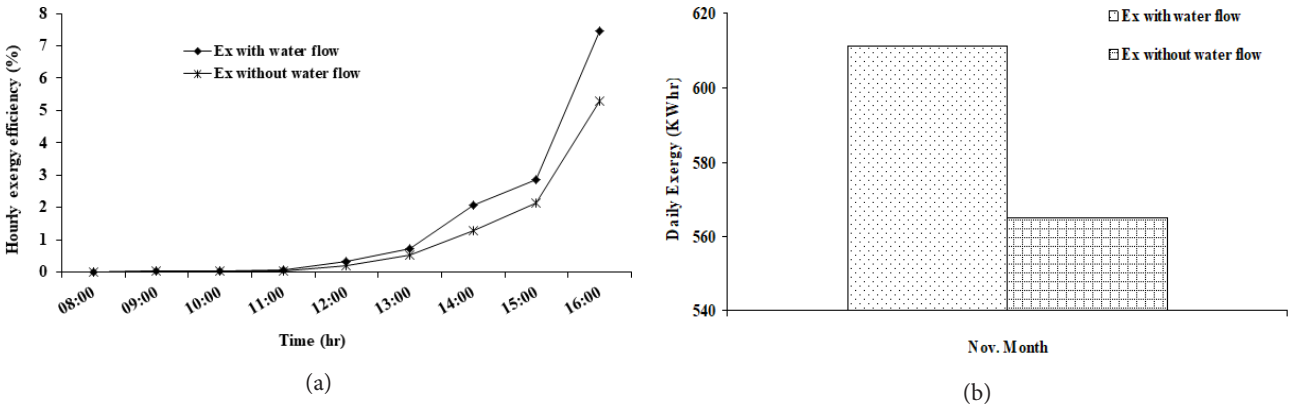

(a) (b)

Figure 8. (a) Variations of hourly exergy efficiency with time. (b) Daily exergy efficiency for month of November.

the HASS is shown in Figures 8a-b. Higher exergy output was reported for the HASS with water flowing over the glass surface and this is due to higher output of daily yield.

Figures 9a–e shows the monthly variation of yield of four different climatic conditions for five climatic zones (i.e. Bangalore, Jodhpur, Mumbai, New Delhi and Srinagar) of India. Figure 9a shows that Bangalore city generates maximum yield for the b climatic condition throughout the year except three months (Mar, Apr and Sept.). It is due to the fact that maximum total number of days is for the b climatic condition and hence total maximum radiations.

The Figures 9b–c shows that for the climatic condition of Jodhpur and Mumbai the monthly yield is maximum for the b climatic condition throughout the year. It is due to the fact that in both cities the b climatic condition prevails almost for half the year, and hence receives maximum radiation. For the New Delhi climatic conditions the monthly yield is maximum for all four climatic conditions but in different months of the year as shown in Figure 9d. It is because of the fact that New Delhi has composite climate and there is large variation in the ambient air temperature throughout the year. Figure 9e shows that at least for six month, monthly yield for the 'a' and 'b' climatic condition is maximum for the Srinagar. It is due the fact that Srinagar has maximum number of days of the 'a' and the 'b' climatic condition (101 and 173 respectively). Srinagar generates the minimum monthly yield in the month of October, November, December and January because of low radiations and minimum ambient air temperature.

Figure 10a shows that for the a and b climatic condition the calculated value of yearly yield is maximum for the Bangalore and Jodhpur respectively but for both the c and the d climatic conditions the value of yearly yield is maximum for the New Delhi climatic zone. From the Figure 10b it is clear that the total annual yield is maximum for the Mumbai climatic condition and minimum for Srinagar climatic condition. The maximum annual yield (2756.67) for the Mumbai climatic condition is due to maximum total annual radiation and the moderate overall ambient air temperature throughout the year which enables solar distillation unit to generate higher temperature difference between basin water and glass surface and hence higher distillate output. The lowest yield for the Srinagar is due to minimum annual radiation and low ambient air temperature throughout the year.

CONCLUSIONS

The following conclusions have been reported on experimental and theoretical results for the given parameters of HASS:

- Calculated values of yield and temperature of basin liner, basin water and glass using developed thermal modeling shows good correlation with the experimental data.
- Efficiency of HASS increases by 4% by flowing water over the glass cover.
- Higher exergy output is reported for this new design of HASS.
- Total yearly yield is maximum (2756.67) for the Mumbai and minimum (1820.22) for the Srinagar climatic conditions.

NOMENCLATURE

A	Area of single PV/T collector, m^2
C_f	Specific heat, J/kgK
F_R	Flow rate factor
h	Convective heat transfer coefficient, $W/m^2°C$
I'(t)	Incident solar intensity on PV integrated flat-plate collector, W/m^2
$I_s(t)$	Incident solar intensity on glass of solar still, W/m^2
I_h	Incident solar intensity on horizontal plane, W/m^2
L	Latent heat of vaporization of water, J/kg

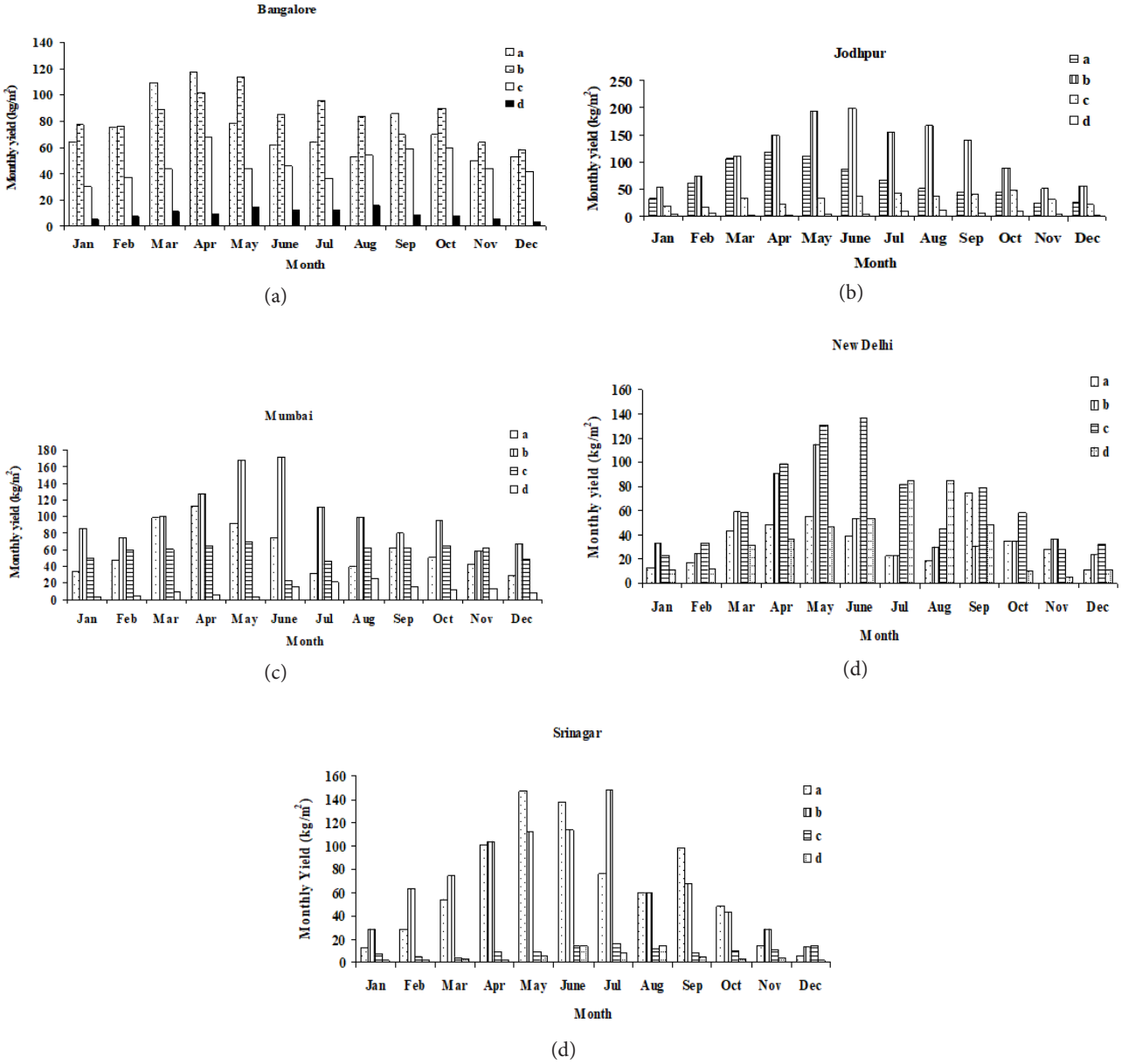

Figure 9. (a) Monthly variation of calculated values of yield for different climatic conditions of Bangalore city. (b) Monthly variation of calculated values of yield for different climatic conditions of Jodhpur city. (c) Monthly variation of calculated values of yield for different climatic conditions of Mumbai city. (d) Monthly variation of calculated values of yield for different climatic conditions of New Delhi city. (e) Monthly variation of calculated values of yield for different climatic conditions of Srinagar city.

$\dot{m}_{ew}$	Distillate output, kg/s
$\dot{m}_{w}$	Mass flow rate of water, kg/s
$\dot{m}_{w2}$	Mass flow rate of water flowing above the glass surface (kg/s)
M_w	Mass of water, kg
PF2	Penalty factor due to the absorber below PV module
$\dot{Q}_u$	Rate of useful energy transfer, kW
$\dot{Q}_{u(m+c1+c2)}$	Thermal energy at the outlet of PV/T collectors, W
$\dot{q}_{ew}$	Heat transfer rate from water surface to condensing cover, W
t	Time interval, s
T	Temperature, °C
U_{Lc}	Overall heat loss coefficient from flat-plate collector to the ambient, W/m²K
$U_{L,m}$	Top heat loss coefficient from solar cell to ambient, W/m²K
V_a	Wind velocity, m/s

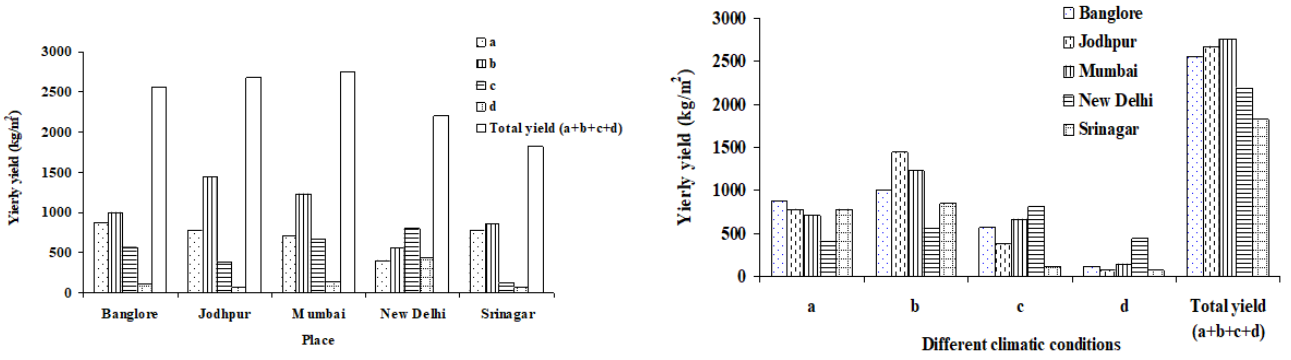

(a) (b)

Figure 10. (a) Calculated values of Yearly yield for different climatic conditions for different climatic zones. (b) Calculated values of Yearly yield for different climatic zones in the various climatic conditions.

Greek symbols

α	Absorptivity
α'	Fraction of solar flux absorbed
σ	Stefan-Boltzmann constant (5.6697×10^{-8} W/m^2 K^4)
ε	Emissivity of glass
τ	Transmitivity

Subscripts

a	Ambient
b	Basin
bw	Basin to water
c	Collector
cw	Water to condensing cover
dest	Destruction
e	Evaporative
eff	Effective
f_i	Inlet fluid
f_o	Outgoing fluid
i	Inner
in	Inflow
g	Glass
m	Module
o	Outer
out	Outflow
p	Plate
r	Radiative
s	Side wall
w	Water
1g	External
1w	Internal
12	Glass to flowing water above the glass surface
1w2	Flowing water to ambient air

AUTHORSHIP CONTRIBUTIONS

Design, Materials, Data Analysis, Writing: M.K. Gaur; Concept: G.N. Tiwari; Critical revision: P. Singh; Literature Search: A. Kushwah.

DATA AVAILABILITY STATEMENT

No new data were created in this study. The published publication includes all graphics collected or developed during the study.

CONFLICT OF INTEREST

The author declared no potential conflicts of interest with respect to the research, authorship, and/or publication of this article.

ETHICS

There are no ethical issues with the publication of this manuscript.

REFERENCES

[1] Yousef MS, Hassan H, Sekiguchi H. Energy, exergy, economic and enviroeconomic (4E) analyses of solar distillation system using different absorbing materials. Appl Therm Eng 2019;150:30–41. [CrossRef]

[2] Taner T, Dalkilic AS. A feasibility study of solar energy-techno economic analysis from Aksaray city, Turkey. J Therm Eng 2019;5:25–30. [CrossRef]

[3] Gurupatham SK, Manikandan GK, Fahad F. Harnessing and storing solar thermal energy using phase change material (PCM) in a small flat plate collector. J Therm Eng 2020;6:511–20. [CrossRef]

[4] Mahian O, Kianifar A, Jumpholkul C, Thiangtham P, Wongwises S, Srisomba R. Solar Distillation Practice For Water Desalination Systems. J Therm Eng 2015;1:287. [CrossRef]

[5] Mohamed AF, Hegazi AA, Sultan GI, El-Said EMS. Augmented heat and mass transfer effect on performance of a solar still using porous absorber: Experimental investigation and exergetic analysis. Appl Therm Eng 2019;150:1206–15. [CrossRef]

[6] Bait O. Exergy, environ–economic and economic analyses of a tubular solar water heater assisted solar still. J Clean Prod 2019;212:630–46. [CrossRef]
[7] Telkes M. Improved Solar Stills. Trans Conf Use Sol Energy. Sci Basis, Tuscon Arizona, Vol. 3, October 31- November 1: 1955:145–53 (Chapter 14, part 2).
[8] Cooper PI. Digital simulation of transient solar still processes. Sol Energy 1969;12:313–31. [CrossRef]
[9] Cooper PI. The maximum efficiency of single-effect solar stills. Sol Energy 1973;15:205–17. [CrossRef]
[10] Dunkle RV. Solar water distillation: the roof type still and a multiple effect diffusion still. Int Heat Transf Conf Colorado, USA. 1961:895–902.
[11] Rahbar N, Esfahani JA. Productivity estimation of a single-slope solar still: Theoretical and numerical analysis. Energy 2013;49:289–97. [CrossRef]
[12] Malik MAS, Tiwari GN, Kumar A, Sodha MS. Solar Distillation: A Practical Study of a Wide Range of Stills and Their Optimum Design, Construction and Performance. 1st ed. Newyork: Pergamon Press, Oxford; 1982.
[13] Tiwari GN, Tiwari A. Solar distillation practice in water desalination systems. Tunbridge Wells, UK: Anshan; 2008.
[14] Kumar S, Tiwari GN. Performance evaluation of an active solar distillation system. Energy 1996;21:805–8. [CrossRef]
[15] Sanjeev K, Tiwari GN. Optimization of daily yield for an active double effect distillation with water flow. Energy Convers Manag 1999;40:703–15. [CrossRef]
[16] Zurigat YH, Abu-Arabi MK. Modelling and performance analysis of a regenerative solar desalination unit. Appl Therm Eng 2004;24:1061–72. [CrossRef]
[17] Sinha S, Kumar. Sanjay. Theoretical evaluation of air regenerative solar distiller integrated with aspirator. Renew Energy 1994;4:311-8. https://doi.org/10.1016/0960-1481(94)90034–5.
[18] Prakash J, Kavathekar AK. Performance prediction of a regenerative solar still. Sol Wind Technol 1986;3:119–25. [CrossRef]
[19] Tiwari GN, Sinha S. Parametric studies of active regenerative solar still. Energy Convers Manag 1993;34:209–18. [CrossRef]
[20] Lawrence SA, Gupta SP, Tiwari GN. Effect of Heat capacity on the performance of solar still with water flow over the glass cover. Energy Convers Manag 1990;30:277–85. [CrossRef]
[21] Singh AK, Tiwari GN. Thermal evaluation of regenerative active solar distillation under thermosyphon mode. Energy Convers Manag 1993;34:697–706. [CrossRef]
[22] Abu-Hijleh BAK. Enhanced solar still performance using water film cooling of the glass cover. Desalination 1996;107:235–44. [CrossRef]
[23] Wibulswa P, Tadtiam S. Improvement of a basin type solar still by means of vertical back wall. Int. Symp. Work. Renew. Energy Sources, Lahore: 1984.
[24] Kudish AI. Water desalination. In: Parker BF, editor. Sol Energy Agric. Amsterdam: Elsevier; 1991:255–94 (Chapter 8).
[25] Wibulswa P, Suntrirat S. No Title. Int. Symp. Work. Renew. Energy Sources, Lahore: 1984.
[26] Gugulothu R, Somanchi NS, Reddy KVK, Gantha D. A Review on Solar Water Distillation Using Sensible and Latent Heat. Procedia Earth Planet Sci 2015;11:354–60. [CrossRef]
[27] Tiwari GN, Madhuri. Effect of water depth on daily yield of the still. Desalination 1987;61:67–75. [CrossRef]
[28] Tsilingiris PT. Theoretical derivation and comparative evaluation of mass transfer coefficient modeling in solar distillation systems - The Bowens ratio approach. Sol Energy 2015;112:218–31. [CrossRef]
[29] Kumar S, Tiwari GN. Estimation of internal heat transfer coefficients of a hybrid (PV/T) active solar still. Sol Energy 2009;83:1656–67. [CrossRef]
[30] Kumar S, Tiwari A. An experimental study of hybrid photovoltaic thermal (PV/T)-active solar still. Int J Energy Res 2008;32:847–58. [CrossRef]
[31] Gaur MK, Tiwari GN. Optimization of number of collectors for integrated PV/T hybrid active solar still. Appl Energy 2010;87:1763–72. [CrossRef]
[32] Singh DB, Tiwari GN. Performance analysis of basin type solar stills integrated with N identical photovoltaic thermal (PVT) compound parabolic concentrator (CPC) collectors: A comparative study. Sol Energy 2017;142:144–58. [CrossRef]
[33] Kabeel AE, Abdelgaied M. Observational study of modified solar still coupled with oil serpentine loop from cylindrical parabolic concentrator and phase changing material under basin. Sol Energy 2017;144:71–8. [CrossRef]
[34] El-Sebaii AA, El-Naggar M. Year round performance and cost analysis of a finned single basin solar still. Applied Thermal Engineering 2017;110:787–94. [CrossRef]
[35] Muthu Manokar A, Prince Winston D, Kabeel AE, El-Agouz SA, Sathyamurthy R, Arunkumar T, et al. Integrated PV/T solar still- A mini-review. Desalination 2018;435:259–67. [CrossRef]
[36] Boubekri M, Chaker A, Cheknane A. Modeling and simulation of the continuous production of an improved solar still coupled with a photovoltaic/thermal solar water heater system. Desalination 2013;331:6–15. [CrossRef]
[37] Singh HN, Tiwari GN. Monthly performance of passive and active solar stills for different Indian climatic conditions. Desalination 2004;168:145–50. [CrossRef]

[38] Arunkumar T, Kabeel AE, Raj K, Denkenberger D, Sathyamurthy R, Ragupathy P, et al. Productivity enhancement of solar still by using porous absorber with bubble-wrap insulation. J Clean Prod 2018;195:1149–61. [CrossRef]
[39] Dubey S, Tiwari GN. Thermal modeling of a combined system of photovoltaic thermal (PV/T) solar water heater. Sol Energy 2008;82:602–12. [CrossRef]
[40] Hepbasli A. A key review on exergetic analysis and assessment of renewable energy resources for a sustainable future. Renew Sustain Energy Rev 2008;12:593–661. [CrossRef]
[41] Petela R. Exergy of undiluted thermal radiation. Sol Energy 2003;74:469–88. [CrossRef]
[42] Kumar S, Tiwari GN. Estimation of convective mass transfer in solar distillation systems. Sol Energy 1996;57:459–64. [CrossRef]

APPENDIX:

For calculating the various parameters of the HASS, following formulas are used:

$$\dot{Q}_{(u,1(m+c))} = \dot{m}_f C_f (T_{fo1} - T_{f1}) \quad \text{(A.1)}$$

here, $T_{fo1} = T_{fi} + \dfrac{\dot{Q}_{u,m}}{\dot{m}_f C_f}$, then

$$\dot{Q}_{u,1(m+c)} = \left[A_m F_{Rm} PF_2 (\alpha\tau)_{m,eff} \left(1 - \frac{A_{c1} F_{Rc1} U_{L,c1}}{\dot{m}_f C_f} \right) + A_{c1} F_{Rc1} (\alpha\tau)_{c1,eff} \right] I'(t) - \left[A_m F_{Rm} U_{L,m} \left(1 - \frac{A_{c1} F_{Rc1} U_{L,c1}}{\dot{m}_f C_f} \right) + A_{c1} F_{Rc1} U_{L,c1} \right] (T_{fi} - T_a) \quad \text{(A.2)}$$

The efficiency factor for the collector is calculated using:

$$F' = \frac{1}{\dfrac{W \times U_L}{\pi D h} + \dfrac{W}{D + (W - D)F}}$$

Where, $F = \dfrac{tanh\left[m(W-D)\right]/2}{\left[m(W-D)\right]/2}$ and $m = \sqrt{\dfrac{U_L}{K\delta}}$

The flow rate factor (F_R) is calculated using:

$$F_R = \frac{\dot{m} C_f}{A_c U_L} \left[1 - exp\left(- \frac{A_c U_L F'}{\dot{m} C_f} \right) \right] \quad \text{(A.3)}$$

The various convective heat transfer coefficients are calculated using Dunkle's correlations [4]

$$h_{cw} = 0.884(\Delta T)^{1/3} \quad \text{(A.4)}$$

Where,

$$\Delta T = [T_w - T_g + (P_w - P_g)(T_w + 273) \times (268.9 \times 10^3 - P_w)^{-1}]^{1/3} \quad \text{(A.5)}$$

$$h_{ew} = 0.01623 \times h_{cw} (P_w - P_g) \times (T_w - T_g)^{-1} \quad \text{(A.6)}$$

$$h_{rw} = \mathcal{E} \times 5.67 \times 10^{-8} [\{(T_w + 273)^4 - (T_g + 273)^4\} \times (T_w - T_g)^{-1}] \quad \text{(A.7)}$$

$$h_{1w} = h_{cw} + h_{ew} + h_{rw} \quad \text{(A.8)}$$

The correlation of vapour pressure in terms of temperature is given by:

$$P_w = exp\left(25.317 - \frac{5144}{T_w + 273} \right)$$

and

$$P_g = exp\left(25.317 - \frac{5144}{T_g + 273} \right)$$

The distillate output is calculated using:

$$\dot{m}_{ew} = \frac{q_{ew} \times A_t \times t}{L} \quad \text{(A.9)}$$

Latent heat of vaporization is given by:
When $T_v > 70°C$,

$$L = 3.1615 \times 10^6 \times [1 - (7.616 \times 10^{-4} \times T_v)] \quad \text{(A.10)}$$

When $T_v < 70°C$,

$$L = 2.4935 \times 10^6 \times [1 - 9.4779 \times 10^{-4} T_v + 1.3132 \times 10^{-7} \times T_v^2 - 4.7974 \times 10^{-9} \times T_v^3] \quad \text{(A.11)}$$

The design parameters of HASS with water flowing over the glass surface are computed using following expressions:

$$\left(\alpha'_{eff}\right) = \left[\alpha'_w + h'_1 \alpha'_g A_g + h_1 \alpha'_b \right]$$

$$h'_1 = \frac{h_{1w}}{h_{12} A_g + h_{1w} A_b}$$

$$h_1 = \frac{h_{bw}}{h_{ba} + h_{bw}}, (UA)_s = A_b [U_t A_g + U_b], U_t = \frac{h_{12} h_{1w}}{h_{12A_g} + h_{1w} A_b},$$

$$U_b = \frac{h_{ba} h_{bw}}{h_{ba} + h_{bw}} \text{ and } \left(UA\right)_g = \left(\frac{h_{1w} A_b h_{12} A_g}{h_{12A_g} + h_{1w} A_b} \right)$$

$h_{ba} = \left[\dfrac{L_b}{k_b} + \dfrac{1}{2.8} \right]^{-1}$ and h_{bw} is 250 W/m^{2}K and 200 W/m^{2}K in months of summer and winter.

The total external heat transfer coefficient is given as:

$$h_{1w2} = h_{cw2} + h_{ew2} + h_{rw2} \quad \text{(A.12)}$$

where,

$$h_{ew2} = 0.01623 \times h_{cw2} (\bar{P}'_{w2} - \gamma \bar{P}_a) \times (\bar{T}'_{w2} - \bar{T}_a)^{-1}$$

$$h_{rw2} = \varepsilon \times 5.67 \times 10^{-8} [\{(\bar{T}'_{w2} + 273)^4 - (\bar{T}_a + 273)^4\} \times (\bar{T}'_{w2} - \bar{T}_a)^{-1}]$$

here $\bar{T}'_{w2}$ and $\bar{T}_a$ are the average of observed value of flowing water and ambient air temperature respectively.

$$h_{cw2} = 2.8 + 3V_a$$

here we have taken h_{cw2} = 3m/s